



Variable Clonal Repopulation Dynamics Influence Chemotherapy Response in Colorectal Cancer

Antonija Kreso *et al.* Science **339**, 543 (2013); DOI: 10.1126/science.1227670

This copy is for your personal, non-commercial use only.

If you wish to distribute this article to others, you can order high-quality copies for your colleagues, clients, or customers by clicking here.

Permission to republish or repurpose articles or portions of articles can be obtained by following the guidelines here.

The following resources related to this article are available online at www.sciencemag.org (this information is current as of February 25, 2013):

Updated information and services, including high-resolution figures, can be found in the online version of this article at:

http://www.sciencemag.org/content/339/6119/543.full.html

Supporting Online Material can be found at:

http://www.sciencemag.org/content/suppl/2012/12/12/science.1227670.DC1.html

A list of selected additional articles on the Science Web sites **related to this article** can be found at:

http://www.sciencemag.org/content/339/6119/543.full.html#related

This article **cites 54 articles**, 14 of which can be accessed free: http://www.sciencemag.org/content/339/6119/543.full.html#ref-list-1

This article has been **cited by** 1 articles hosted by HighWire Press; see: http://www.sciencemag.org/content/339/6119/543.full.html#related-urls

This article appears in the following **subject collections**: Medicine, Diseases

http://www.sciencemag.org/cgi/collection/medicine

A prominent but transient authigenic carbonate sink may also help explain carbon isotope variations in the Paleozoic (8, 35) and Early Triassic (36). In the Triassic, for example, there is evidence for widespread anoxia in intermediate waters (37), fluctuating $\delta^{13}C_{carb}$ values (–2 to +8‰), and gradients in the $\delta^{13}C_{carb}$ values with depth, often with δ^{13} C values on the slope 2 to 3‰ lighter than those on the shelf (38). We view the Early Triassic as a candidate for a period of sustained, high authigenic carbonate formation, like much of the Neoproterozoic (23). The fluctuations could be produced either from a change in the global amount of authigenic carbonate (category 1) or by migration in the zone of authigenic carbonate (category 2). In the Early Cambrian, similar fluctuations in the authigenic carbonate sink might have resulted from more modest variations in surface redox or evolutionary leaps such as the biological irrigation of sediments.

The recognition of authigenic carbonate in the sedimentary record presents a challenge for carbon isotope stratigraphy because it allows for local variations in $\delta^{13}C_{carb}$ produced by the addition of a substantial authigenic component after burial. Until there is a clear way to quantify the amount of marine carbonate precipitated in the water column relative to authigenic carbonate precipitated in sediments, questions about the fidelity of chronostratigraphic correlations will remain. Authigenic events are likely to be broadly correlative owing to global changes in surface redox conditions, surface saturation state, and/or eustatic sea level, all of which might drive a migration of the zone of authigenesis or a change in the amount of authigenic precipitation, but detailed correlations at finer scales may prove less reliable.

Including a third major sink for carbon in sedimentary reservoirs does not sever the connection between $\delta^{13}C_{carb}$ and the redox evolution of the Earth surface, but it does imply a more complex relationship. Rather than massive changes in atmospheric O2 and CO2, our framework explains the large variations in $\delta^{13}C_{carb}$ in terms of changes in the amount of authigenic carbonate driven perhaps by small changes in atmospheric O₂ but potentially also by changes in the other redox budgets (SO₄ and Fe), in the strength or even existence of a lysocline, or in the focusing of organic carbon burial in different sedimentary environments. With this new framework, the challenge remains to use the geologic record to understand the driving forces and events that have shaped Earth's surface.

References and Notes

- 1. H. C. Urey, Science 108, 489 (1948).
- 2. W. S. Broecker, J. Geophys. Res. 75, 3553 (1970).
- 3. The inputs of carbon to Earth's surface carbon reservoirs include the return flux of CO₂ from subduction or metamorphic release of carbon from carbonate and organic matter, the outgassing of mantle carbon, and the weathering of carbonate and organic matter. For a more complete discussion, see (39).
- A. H. Knoll, J. M. Hayes, A. J. Kaufman, K. Swett,
 I. B. Lambert, *Nature* 321, 832 (1986).
- J. M. Hayes, H. Strauss, A. J. Kaufman, Chem. Geol. 161, 103 (1999).
- 6. R. A. Berner, Am. J. Sci. 309, 603 (2009).

- 7. L. R. Kump et al., Science 334, 1694 (2011).
- 8. M. R. Saltzman *et al.*, *Proc. Natl. Acad. Sci. U.S.A.* **108**, 3876 (2011).
- 9. F. A. Macdonald et al., Science 327, 1241 (2010).
- G. P. Halverson, P. F. Hoffman, D. P. Schrag, A. C. Maloof, A. H. N. Rice, Geol. Soc. Am. Bull. 117, 1181 (2005).
- 11. D. C. Catling, M. W. Claire, *Earth Planet. Sci. Lett.* **237**, 1 (2005)
- 12. T. F. Bristow, M. J. Kennedy, Geology 36, 863 (2008).
- D. P. Schrag, R. A. Berner, P. F. Hoffman,
 G. P. Halverson, Geochem. Geophys. Geosyst. 3, 1036 (2002).
- C. J. Bjerrum, D. E. Canfield, Proc. Natl. Acad. Sci. U.S.A. 108, 5542 (2011).
- T. H. Naehr et al., Deep Sea Res. Part II Top. Stud. Oceanogr. 54, 1268 (2007).
- 16. H. H. Roberts, P. Aharon, Geo-Mar. Lett. 14, 135 (1994).
- 17. P. Meister et al., Sedimentology 54, 1007 (2007).
- C. E. Reimers, K. C. Ruttenberg, D. E. Canfield, M. B. Christiansen, J. B. Martin, Geochim. Cosmochim. Acta 60, 4037 (1996).
- 19. L. G. Anderson, D. Dyrssen, J. Skei, *Mar. Chem.* **20**, 361 (1987).
- 20. Z. Zhu, R. C. Aller, J. Mak, Cont. Shelf Res. 22, 2065 (2002).
- R. C. Aller, N. E. Blair, Q. Xia, P. D. Rude, Cont. Shelf Res. 16, 753 (1996).
- N. Chow, S. Morad, I. S. Al-Aasm, J. Sediment. Res. 70, 682 (2000).
- J. A. Higgins, W. W. Fischer, D. P. Schrag, *Earth Planet. Sci. Lett.* **284**, 25 (2009).
- A. Prokoph, G. A. Shields, J. Veizer, *Earth Sci. Rev.* 87, 113 (2008).
- G. Jiang, A. J. Kaufman, N. Christie-Blick, S. Zhang, H. Wu. Earth Planet. Sci. Lett. 261, 303 (2007).
- 26. B. Shen et al., Geochim. Cosmochim. Acta 75, 1357 (2011).
- 27. Bjerrum and Canfield (40) derived a similar expression for the addition of carbonate derived from carbonatization reactions in seafloor basalt. The mathematical expression is identical, but the isotopic fractionation for carbonatization is much smaller and hence provides a much smaller

lever to affect the global carbon isotope mass balance. A more complete expression would include separate terms for carbonate in carbonatized basalts as well, provided that they represent removal of carbon from seawater rather than carbon from volcanic outgassing that was never counted in the surface budget.

- 28. O. Sivan, D. P. Schrag, R. W. Murray, *Geobiology* **5**, 141 (2007).
- J. P. Grotzinger, D. A. Fike, W. W. Fischer, *Nat. Geosci.* 4, 285 (2011).
- D. T. Johnston, F. A. Macdonald, B. C. Gill, P. F. Hoffman,
 D. P. Schrag, *Nature* 483, 320 (2012).
- The absence of covariation of the δ¹³C of organic carbon may also be explained by contamination with a secondary component, such as detrital organic carbon (30).
- 32. L. A. Derry, Earth Planet. Sci. Lett. 294, 152 (2010).
- 33. L. P. Knauth, M. J. Kennedy, Nature 460, 728 (2009).
- 34. S. M. A. Duguid, T. K. Kyser, N. P. James, E. C. Rankey, J. Sediment. Res. **80**, 236 (2010).
- 35. A. C. Maloof et al., Geol. Soc. Am. Bull. 122, 1731 (2010).
- 36. J. L. Payne et al., Science 305, 506 (2004).
- A. H. Knoll, J. A. Babcock, J. L. Payne, S. B. Pruss,
 W. W. Fischer, *Earth Planet. Sci. Lett.* **256**, 295 (2007).
- K. M. Meyer, M. Yu, A. B. Jost, B. M. Kelley, J. L. Payne, *Earth Planet. Sci. Lett.* **302**, 378 (2011).
- J. M. Hayes, J. R. Waldbauer, *Phil. Trans. R. Soc. B* 361, 931 (2006).
- C. J. Bjerrum, D. E. Canfield, Geochem. Geophys. Geosys.
 Q08001 (2004).

Acknowledgments: The paper benefited from reviews from J. Hayes, R. Aller, and an anonymous reviewer. The authors acknowledge P. Hoffman for his helpful comments. This work was supported by NSF grant OCE-0961372 to D.P.S. and a Canadian Institute for Advanced Research Junior Fellowship to J.A.H. D.P.S. also thanks the Henry and Wendy Breck Foundation for support.

31 August 2012; accepted 12 December 2012 10.1126/science.1229578

Variable Clonal Repopulation Dynamics Influence Chemotherapy Response in Colorectal Cancer

Antonija Kreso,^{1,2}* Catherine A. O'Brien,^{1,3}* Peter van Galen,¹ Olga I. Gan,¹ Faiyaz Notta,^{1,2} Andrew M. K. Brown,⁴ Karen Ng,⁴ Jing Ma,⁵ Erno Wienholds,¹ Cyrille Dunant,⁶ Aaron Pollett,⁷ Steven Gallinger,⁸ John McPherson,⁴ Charles G. Mullighan,⁵ Darryl Shibata,⁹ John E. Dick^{1,2}†

Intratumoral heterogeneity arises through the evolution of genetically diverse subclones during tumor progression. However, it remains unknown whether cells within single genetic clones are functionally equivalent. By combining DNA copy number alteration (CNA) profiling, sequencing, and lentiviral lineage tracking, we followed the repopulation dynamics of 150 single lentivirus-marked lineages from 10 human colorectal cancers through serial xenograft passages in mice. CNA and mutational analysis distinguished individual clones and showed that clones remained stable upon serial transplantation. Despite this stability, the proliferation, persistence, and chemotherapy tolerance of lentivirally marked lineages were variable within each clone. Chemotherapy promoted the dominance of previously minor or dormant lineages. Thus, apart from genetic diversity, tumor cells display inherent functional variability in tumor propagation potential, which contributes to both cancer growth and therapy tolerance.

ancer is sustained by production of aberrant cells that vary in many morphological and physiological properties. This cellular diversity remains a major challenge to our understanding of the neoplastic process and therapeutic resistance. Genetic and nongenetic processes can generate heterogeneity; however, the degree of coordination between these mechanisms and their relative contribution to tumor propagation remains unresolved.

Tumor cell diversity can arise through accrued genetic changes (I) that result in single tumors composed of many subclones that develop through complex evolutionary trajectories (2, 3). As well, tumors contain genetic subclones that vary with respect to differential growth in xenograft assays (4-6), recurrence (7), and metastatic potential (8, 9). Likewise, resistance to cancer therapies can arise through genetic mutations (10, 11).

These and other studies substantiate the widely accepted view that tumors comprise genetically diverse subclones, some of which survive therapy and contribute to disease recurrence.

In the absence of differences at the level of genetic mutation, heterogeneity within a population of tumor cells can still exist, but the mechanisms remain incompletely understood. For example, the bidirectional interaction between tumor cells and the microenvironment can influence tumor phenotype (12). Other processes have also been proposed, including interconvertible activation of Rac and Rho guanosine triphosphatases (13), metastable configurations of intracellular networks (14, 15), and altered epigenetic states (16). These studies collectively indicate that in apparently homogeneous in vitro environments, cells of the same genotype can exist in different states that influence their behavior (17). The detection of in vitro cellular diversity, which is not coupled to genetic diversity, underscores the need to investigate the extent of intraclonal functional heterogeneity in vivo and in primary human cancers.

Arguably the most important function of any cancer clone is to maintain long-term tumor propagation. For many tumors, only a minority of cells are able to sustain tumor growth, although such cells can constitute the majority of tumor cells for some cancer types (18, 19). Whether these cells are part of one genetic clone or are derived from distinct genetic subclones remains to be determined. Moreover, whether tumor-propagating cells of a single genetic clone are all equivalent or whether there is functional variability among individual tumor cells is uncertain. Addressing these questions requires genetic analyses combined with functional assays that measure tumor propagation at the resolution of individual clones derived from single cells.

Clonal stability is maintained through serial tumor transplantation. To explore the relative contribution of genetic and nongenetic mechanisms to the functional heterogeneity of single human cancer cells that are capable of long-term clonal propagation, we used an in vivo xenotransplantation assay. The fates of single cell-derived lineages were tracked from 10 primary human colorectal cancers (CRCs; table S1). To facilitate clonal tracking, we transduced patient-

derived CRC cells with a green fluorescent protein (GFP)-expressing lentivirus and injected the cells into the renal capsule of immunodeficient mice (supplementary text and tables S2 and S3). Transduced cells efficiently generated xenografts, and GFP expression in the xenografts remained stable over serial transplantation (figs. S1 and S2). The average time to palpable tumor formation (99 ± 18 days) was stable over serial transplants (Fig. 1A), and xenografts maintained patient tumor characteristics (figs. S3 to S5). Genomic profiling of three patient tumors and corresponding xenografts using copy number alteration (CNA) analysis (Fig. 1B, figs. S6 and S7, and table S4) and targeted deep sequencing of 660 mutational hotspots in 42 genes (Fig. 1C and tables S5 to S7) established that xenografts largely retained the genomic profile of the primary tumor sample. Several CNAs and singlenucleotide variants (SNVs) were enriched in primary 1° xenografts from some samples, consistent with selection of a subclone from the patient tumor. Genomic analysis of subsequent xenograft transplants, encompassing 393 days (patient sample CT38), 341 days (CT54), and 261 days (CT59) of total tumor growth, demonstrated that the majority of genomic lesions detected in 1° xenografts were recapitulated upon serial passage (supplementary text). Exome sequencing of CT38 and its corresponding 1°, 2°, and 4° xenografts supported these findings (supplementary text, figs. S8 and S9, and tables S8 to S11). Finally, analysis of methylation pattern diversity of patient tumors and their corresponding xenografts indicated that population diversity was maintained over serial passage (supplementary text and fig. S10). Collectively, these data indicate that the CRC clones that are selected in the xenograft remain stable over sequential transplantation.

Variation in clonal dynamics of CRC cells. To evaluate the repopulation kinetics of multiple single cell—derived clones within a primary human tumor, we used lentiviral marking to track the progeny of single CRC cells (henceforth termed "LV clones" to distinguish them from genetic clones) over serial xenografts. To facilitate qualitative and quantitative characterization, we developed a system for establishing clonal identity and then classifying clonal behavior according to persistence, absence, or emergence across multiple recipients (see supplementary text). Rather than relying on the polymerase chain reaction, our detection strategy focused on the identification of LV clones that possessed robust clonal expansion capacity.

We observed five distinct behaviors. LV clones that were present in all serial transplants were termed type I or persistent clones (Fig. 2A, purple arrowhead). LV clones that did not persist but exhausted before reaching the final passage had less potent tumor-propagating ability relative to type I clones; these were termed type II or short-term clones (Fig. 2A, blue arrowhead). Finally, we observed LV clones that lacked tumor-propagating ability because they were only detected in the 1° recipient and were not detected in 2° and subse-

quent recipients (Fig. 2A, green arrowhead); these were termed type III or transient clones. In 10 patient samples, out of a total of 150 marked clones, we tracked 34 type I, 33 type II, and 31 type III clones (Fig. 2B), which suggests that there is substantial functional diversity with respect to clonal longevity in successive tumor transplants.

In addition to heterogeneity in longevity, we also observed dynamic behaviors in 34 of the 150 marked clones. These LV clones were initially below detection limits (approximately 10⁴ cells/ tumor) in the 1° recipients but could be identified at later transplants (Fig. 2A, red arrowhead). Because the xenograft assay monitors the output of "active" CRC cells, these type IV or resting LV clones were likely produced by CRC cells that initially were dormant or slowly proliferated but became activated in later transplants, resulting in the generation of a measurable clone. Finally, LV clones whose progeny appeared early, then became undetectable in a subsequent transplant, only to reappear at a later time point (Fig. 2A, orange arrowhead) were termed type Vor fluctuating clones. Such LV clones displayed extensive but intermittent proliferation distinct from the continuous rapid proliferation of type I clones; we observed 18 examples of type V clones (Fig. 2B). Overall, these results show that not all CRC cells with the potential for tumor propagation actually function and contribute to tumor growth at any given time. Such cells can become activated at later time points.

It is noteworthy that LV clones can remain undetected for 2 to 4 months while being diluted by a factor of >100 during consecutive transplants and then recur to dominate tumor growth (supplementary text and fig. S11). Whereas random growth dynamics would predict dilution of minor LV clones over multiple transplants, the frequent detection of type IV and V clones indicates that the behaviors we observe cannot be solely attributed to dilution over time or stochasticity in LV clonal behaviors. Further, mathematical modeling also predicted that LV clonal emergence correlates with changes in tumor structure and that newly appearing clones are functionally distinct from active clones, although it did raise uncertainty as to whether types I, II, and III are distinct or whether stochastic processes related to the transplantation method may contribute to clonal loss (supplementary text and fig. S12). The distinct proliferative kinetics of the five LV clonal behaviors we observed underscore the functional variability of individual cells (Fig. 2C). Each LV clone type was identified in four or more patient samples (Fig. 2D and fig. S13), establishing that the varied clonal behaviors are reproducibly found in primary CRC from a spectrum of patients. Given the absence of accompanying changes in CNAs and SNVs with serial transplantation, our data provide evidence for functional heterogeneity between individual tumor-propagating cells that share a common genetic lineage.

The genetic analysis across xenografts was carried out on bulk tumor cell populations, where clonal marking tracked the functional behavior

¹Campbell Family Institute, Ontario Cancer Institute, Princess Margaret Cancer Centre, University Health Network, Toronto, Ontario M5G 117, Canada. ²Department of Molecular Genetics, University of Toronto, Toronto, Ontario M5G 1L7, Canada. ³Department of Laboratory Medicine and Pathobiology and Department of Surgery, University of Toronto, Toronto, Ontario M5L 1F4, Canada. ⁴Ontario Institute for Cancer Research, Toronto, Ontario M5G 1L7, Canada. ⁵St. Jude Children's Hospital, Memphis, TN 38105, USA. ⁶Department of Civil Engineering, University of Toronto, Toronto, Ontario M5S 1A4, Canada. ⁷Department of Pathology, Mount Sinai Hospital, Toronto, Ontario M5G 1X5, Canada. ⁸Fred Litwin Centre for Cancer Genetics, Samuel Lunenfeld Research Institute, Mount Sinai Hospital, Toronto, Ontario M7H 2B9, Canada. ⁹University of Southern California Keck School of Medicine, Los Angeles, CA 90089, IISA

^{*}These authors contributed equally to this work. †To whom correspondence should be addressed. E-mail: jdick@uhnres.utoronto.ca

of single cells. The experimental design of genomically analyzing bulk tumor does not directly evaluate the genomic properties of each individual functionally distinct LV clone type that is present. To directly compare the genomes of distinct LV clone types from an individual tumor, we used a limiting dilution approach to isolate different LV clones and used deep sequencing of mutational hotspots to compare their mutational load. We compared the mutational hotspots between tumors generated by a type I and type V clone from CT38 and a type I and type II clone from CT59. For CT38, a linear correlation between the SNV frequencies of the type I- and type V-derived tumors was seen (fig. S14A and table S12). Likewise, for CT59, type I- and type

II-derived tumors also demonstrated similar SNV frequencies in all analyzed SNVs, including the nine somatically acquired SNVs (fig. S14B and table S13). Thus, for both CT38 and CT59, the frequency of analyzed hotspot mutations was congruent between tumors generated by single LV clones, which were derived from distinct clone types (type I and V for CT38; type I and II for CT59). Analyzing tumors generated from single cells enabled us to determine that distinct clone types within a tumor sample share similar mutational patterns as assessed by targeted sequencing. These data, together with the CNA and targeted sequencing analysis of the bulk tumor, provide further evidence for the existence of functionally distinct LV clones within a genetic lineage in CRC.

Variable response of LV clones to oxaliplatin.

The existence of functionally heterogeneous CRC cells prompted us to investigate whether these cells might also intrinsically differ in response to therapy. We examined the effect of a commonly used chemotherapy drug, oxaliplatin, on the dynamics of LV clones. We used established xenografts of five patient samples for which the LV clone types had already been curated. In parallel with the serial transplantation of untreated recipient mice described above, three to five additional mice were transplanted with tumor cells and systemically treated with oxaliplatin once tumors were established, allowing assessment of the effects of drug treatment on steady-state clonal distribution (fig. S15A). Although oxaliplatin

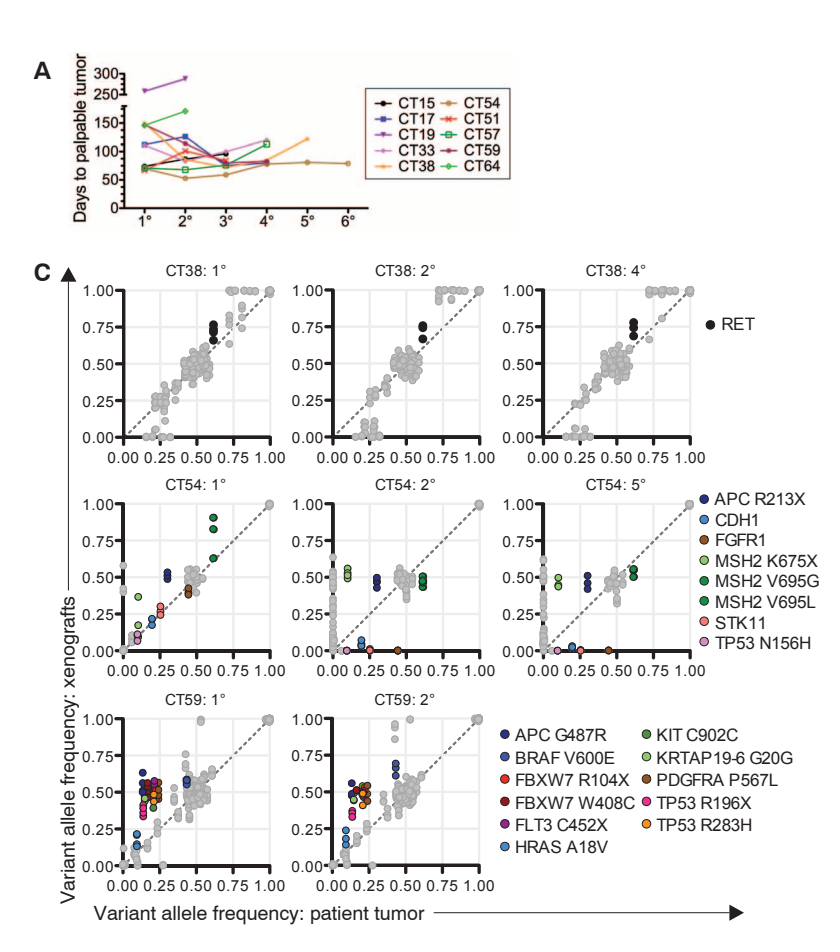
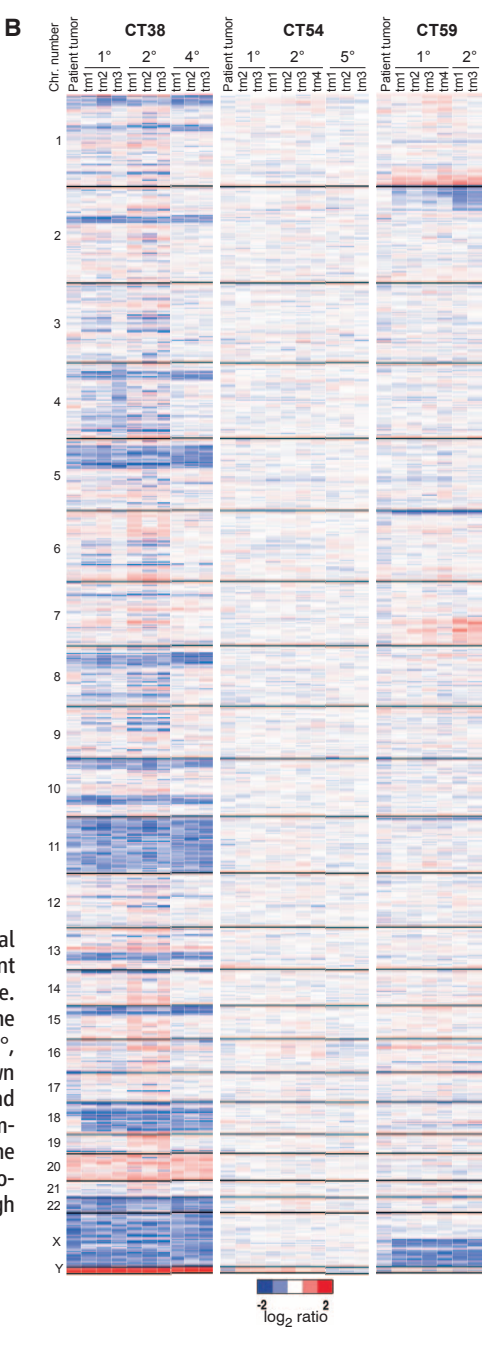


Fig. 1. Xenograft characterization. **(A)** Diagnostic tumor samples were transduced with a lentiviral vector encoding GFP, and 5×10^4 to 2×10^5 viable cells were transplanted into immunodeficient mice. Once tumors formed (1°), an equal number of cells was transplanted into the next passage. Time to tumor formation from previous injection for each transplant is shown. Each point is the mean of all recipients at the indicated passage. **(B)** DNA from diagnostic and matching 1°, 2°, 4°, and 5° tumor transplants was profiled using Affymetrix SNP 6.0 arrays. Raw \log_2 ratios are shown (median smoothing format; blue, deletion; white, normal; red, gain). **(C)** DNA from diagnostic and xenograft derived tumors was sequenced using the RainDance platform. Frequency of both germline (gray circles) and somatic variants (colored circles) is shown. Each circle represents data of one xenograft-derived tumor as compared to the patient tumor sample; there are three or four xenografts per passage. Data are not normalized for copy number changes and tumor cellularity, although generally >80% of cells are estimated to be tumor cells.



treatment reduced tumor burden (figs. S15B and S16A), there was no apparent change in the absolute number of marked clones (fig. S15C), nor were the proportions of clone types significantly altered (figs. S15D and S17).

To determine whether treatment with oxaliplatin affected CRC cells with tumor propagation capability, we serially transplanted equal numbers of viable cells from both the control and treatment groups into secondary mice that were left untreated. Across five patient samples, a total of 60 secondary recipients were transplanted with tumor cells from oxaliplatin-treated xenografts (31 control and 29 oxaliplatin-treated). We observed a reduction in tumor weight (Fig. 3A and fig. S16B), as well as a trend toward a decrease in the absolute number of clones (Fig. 3B), in un-

treated secondary recipients transplanted with cells from oxaliplatin-treated xenografts versus shamtreated control cells; these results suggested that drug treatment altered the growth properties of the regrown tumor. For two samples (CT33 and CT57), GFP-expressing tumor tissue was not detected in the secondary recipients that were transplanted with oxaliplatin-treated cells, which precluded lentiviral insertion site analysis. For the remaining three patient samples (CT17, CT38, and CT54), major changes in the proportion of LV clone types occurred in xenografts derived from the oxaliplatintreated group relative to control xenografts (Fig. 3C). The proportion of type I persistent clones was reduced, whereas LV clones that were below the detection limit in primary recipients appeared in secondary recipients transplanted with oxaliplatin-

treated tumors (Fig. 3D; Fig. 3E, arrowheads to the right). These new LV clones were classified as type IV because they were not consistently detected in control or oxaliplatin-treated tumors in preceding mice. When considering the absolute numbers of different LV clone types over the complete set of secondary mice, 84 type I clones were observed in mice transplanted with untreated control cells and 27 type I clones in mice transplanted with oxaliplatin-treated cells (Fig. 3D). By contrast, 12 type IV clones were detected in the control group versus 40 type IV clones in the oxaliplatin-treated group. These data indicate that the response of individual CRC cells to standard chemotherapy is markedly variable. Despite eradication of some persistent LV clones, resting or slowly proliferating CRC cells can endure

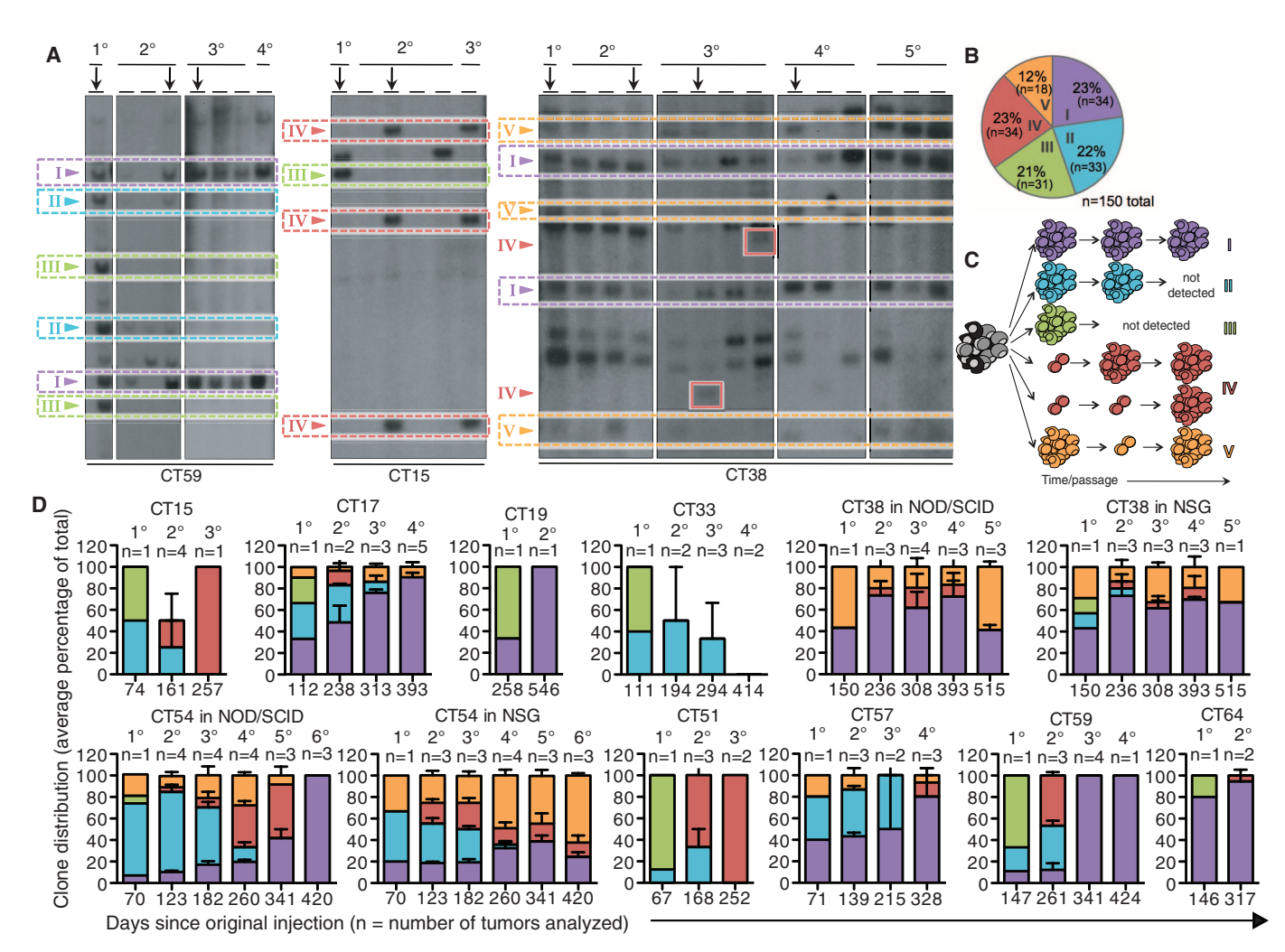


Fig. 2. Variation in repopulation potential of individual lentivirally-marked CRC cells. **(A)** DNA from xenografts (one tumor per lane) of various transplants (denoted by 1°, 2°, ..., 5°) was analyzed using Southern blotting with a GFP probe. Arrows above certain lanes indicate the tumor that was retransplanted into the next set of mice. Colored arrowheads indicate representative examples of different lentivirally marked (LV) clone types. **(B)** Pie chart showing the sum of each of the five LV clone types observed over all experiments. **(C)** Schematic illustrating the different types of LV clonal behaviors. LV clones were classified on the basis of detection in serial transplants; for example, a type IV clone would be below the detection limit initially and come up in later

transplants. **(D)** Charts showing the proportion of LV clone types for each patient sample, displayed as the averages of all mice per transplant. The proportion of each LV clone type was determined in every recipient mouse by dividing the number of times a particular LV clone type was observed by the total number of LV clones detected in that mouse, thereby normalizing for differential marking of samples. Next, the proportion of each LV clone type for all recipients per transplant was averaged, including recipients for which LV clones were not detected. Each bar is representative of the averaged data at a transplant, and error bars indicate SEM between the tumors; *n* denotes the number of tumors or recipients analyzed.

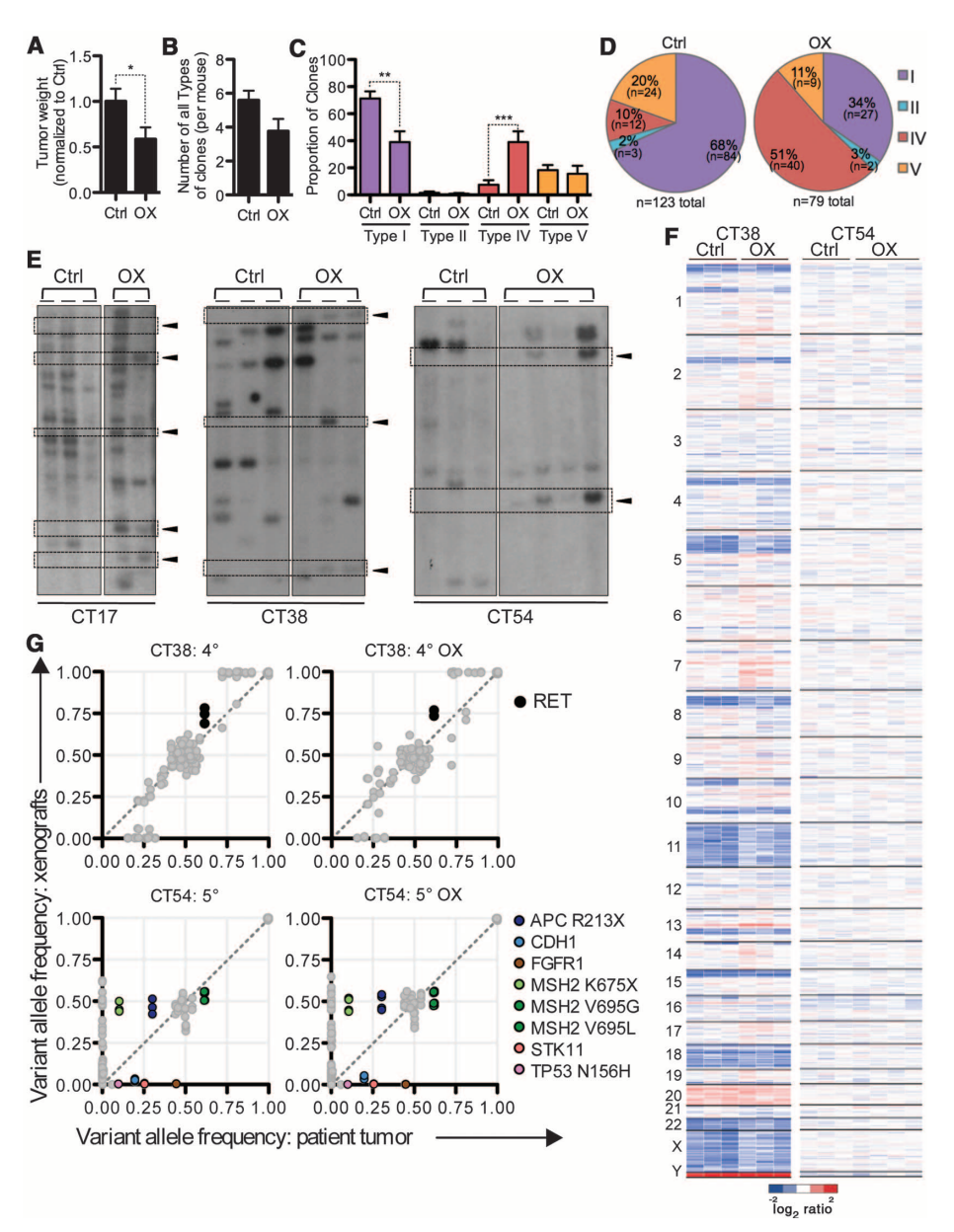


Fig. 3. Variable response of marked clones to oxaliplatin. Mice were either treated with phosphatebuffered saline (Ctrl) or oxaliplatin (OX) for 2 to 4 weeks and cells from these tumors were reinjected into mice, which did not receive further treatment. Once new tumors formed (about 100 days after reinjection), mice from both groups were killed and tumor weight was measured. (A) Previously OXtreated tumor weights were normalized to Ctrl tumor weights; data were pooled from five patient samples representing 31 Ctrl and 29 previously OX-treated samples. (B) Cumulative number of LV clones per mouse after transplantation of OX-treated tumors. (C) The proportion of LV clone types in tumors that were generated by reinjecting Ctrl and OX-treated tumors. LV clone types were assigned according to the behavior of individual clones across all transplants over the entire experiment. Data are means ± SEM of pooled data from independent OX treatments using different patient samples; P values were calculated using two-tailed t test. (**D**) Pie chart showing the number of times the LV clone types were observed, represented as the sum of all experiments. (E) Southern blot showing the LV clonal makeup of tumors generated by reinjecting tumor cells from OX-treated recipients. Representative data from three patient samples are shown; solid arrowheads to the right of each experiment identify newly appearing LV clones in the previously OX-treated tumors. Each lane represents the DNA of one mouse. For comparative purposes, the Southern blot for CT38 Ctrl is the same as in Fig. 2A. (F and G) DNA from tumors that were generated by reinjecting Ctrl or OX-treated samples was analyzed using CNA arrays (F) or targeted deep sequencing (G). In (F), raw log₂ ratio copy number data are shown in median-smoothing format (blue, deletion; white, normal; red, gain). For comparative purposes, data for Ctrl in (F) and (G) are reproductions of 4° (CT38) and 5° (CT54) transplants from Fig. 1, B and C.

oxaliplatin treatment and reinitiate tumor growth, although such tumors are of smaller size. Interestingly, mathematical modeling predicted that the LV clonal landscape of post-treatment tumors was distinct from that of untreated samples (supplementary text and fig. S12).

To determine whether the altered clonal patterns after oxaliplatin treatment were due to major changes in genetic clones, we profiled DNA from control and oxaliplatin-treated tumors by genomewide CNA analysis (Fig. 3F), targeted deep sequencing (Fig. 3G), and passenger methylation analysis (fig. S10). The results indicated that the CNAs, SNVs, and methylation pattern diversity of the oxaliplatin-treated group closely matched the control recipients (supplementary text). The absence of a detectable bottleneck or selection for novel genetic clones after chemotherapy treatment indicates that therapeutic tolerance is not always linked to the acquisition of new driver mutations. Instead, variable tumor propagation behavior of individual cells can represent a nongenetic determinant of tumor growth after therapy.

Discussion. Our findings establish that individual tumor cells within a uniform genetic lineage are functionally heterogeneous: They display extensive variation in growth dynamics, persistence through serial transplantation, and response to therapy. Not all functionally important cells contribute continuously to tumor growth; some are held in reserve, while others are able to oscillate between periods of dormancy and activity. This distinct intraclonal behavior affected response to conventional chemotherapy; actively proliferating progeny were preferentially eliminated, whereas the relatively dormant CRC cells became dominant during tumor reinitiation after chemotherapy. The intraclonal diversity in single-cell functional behavior of primary human CRC cells in vivo has the net effect of contributing to tumor growth during both homeostasis and therapy response.

Most tumors are expected to consist of genetically distinct subclones that contain different growth characteristics and will therefore read out differently in xenotransplantation assays (1). Similar to published work using CRC cells propagated in immunodeficient mice (20), we expanded and sequentially propagated CRC clones from different patient samples that remained stable upon serial transplantation, indicating that xenografting does not select for a significantly different tumor cell population between multiple recipients at each stage of serial transplant. Despite this stability, we observed reproducible differences in the functional fates of single marked CRC cells, indicating that in vivo dynamics of lentivirally tracked CRC clones are not driven by readily detectable genomic changes. This conclusion is supported by the genetic concordance between functionally distinct LV clone types within a single tumor isolated by limiting dilution. Thus, in addition to the widely accepted mechanism of tumor heterogeneity being driven by genetic diversity, other diversitygenerating processes exist within a genetic clone. These processes endow cells with robust survival potential, especially during stress. The contribution of diversity-generating mechanisms such as epigenetic regulation, noise in gene expression, or variability in the microenvironment (21, 22) may offer insight into CRC cell heterogeneity.

There is growing evidence of evolutionary selection for diversity-generating mechanisms in other disciplines, such as ecology (23, 24) and microbiology (25-27). For example, genetically homogeneous pools of single-cell prokaryotes display heterogeneity, where a small portion of cells naturally display drug resistance that is not caused by genetic mutation or acquisition of plasmids encoding antibiotic resistance genes. Rather, this phenomenon is due to mechanisms that reduce cell proliferation and induce a dormant nondividing state (28). We consistently observed a relatively dormant cell population in CRC, which suggests that cancer cells may take advantage of this "ancient" mechanism and use dormancy as an adaptive strategy during times of stress. We provide evidence for a relatively dormant or slowly proliferating cell population in primary human CRC cells that still retains potent tumor propagation potential, thereby preferentially driving tumor growth after chemotherapy. These findings may provide a biological basis for recurrent and metastatic disease following standardof-care treatment (29). Our findings should focus efforts to uncover the molecular mechanisms driving chemotherapeutic tolerance in CRC cells.

The often unstated assumption in considering cellular response to stress is that cells react in a uniform manner to the inducing signal, because the classical techniques used bulk populations. However, averaging data across millions of cells has the effect of masking any heterogeneity that might exist at the single-cell level. Such conventions are changing as methodological advances (30) are fueling a surge of interest in the processes governing cell-to-cell variability (14). By coupling genetic analysis to functional tumor growth assays, we find that when cells are tracked at singlecell resolution while still being part of a population of cancer cells, variable cellular behaviors can be detected. These observations set a precedent for future studies examining the basis of intraclonal behavior of single cells, especially with respect to tumor propagation and other functional properties. In a broader sense, our findings reveal another layer of complexity, beyond genetic diversity, that drives the intratumoral heterogeneity of CRC. The prospect of understanding how genetic and nongenetic determinants interact to influence the functional diversity and therapy response for other cancers should drive future cancer research.

References and Notes

- 1. M. Greaves, C. C. Maley, Nature 481, 306 (2012).
- 2. S. Nik-Zainal et al.; Breast Cancer Working Group of the International Cancer Genome Consortium, Cell 149, 994 (2012).
- 3. M. Gerlinger et al., N. Engl. J. Med. 366, 883 (2012).
- 4. K. Anderson et al., Nature 469, 356 (2011).
- 5. F. Notta et al., Nature 469, 362 (2011).
- 6. E. Clappier et al., J. Exp. Med. 208, 653 (2011).
- 7. C. G. Mullighan et al., Science 322, 1377 (2008).
- 8. X. Wu et al., Nature 482, 529 (2012).
- 9 W Liu et al. Nat Med 15 559 (2009)
- 10. M. E. Gorre et al., Science 293, 876 (2001).
- 11. C. Roche-Lestienne, J. L. Laï, S. Darré, T. Facon, C. Preudhomme, N. Engl. J. Med. 348, 2265 (2003).
- 12. M. J. Bissell, M. A. Labarge, Cancer Cell 7, 17 (2005).
- 13. V. Sanz-Moreno et al., Cell 135, 510 (2008).
- 14. S. L. Spencer, S. Gaudet, J. G. Albeck, J. M. Burke,
- P. K. Sorger, Nature 459, 428 (2009). 15. A. Roesch et al., Cell 141, 583 (2010).
- 16. S. V. Sharma et al., Cell 141, 69 (2010).
- 17. P. B. Gupta et al., Cell 146, 633 (2011).
- 18. K. Ishizawa et al., Cell Stem Cell 7, 279 (2010).
- 19. P. N. Kelly, A. Dakic, J. M. Adams, S. L. Nutt, A. Strasser, Science 317, 337 (2007).

- 20. S. Jones et al., Proc. Natl. Acad. Sci. U.S.A. 105, 4283 (2008)
- 21. A. Marusyk, V. Almendro, K. Polyak, Nat. Rev. Cancer 12,
- 22. M. Kærn, T. C. Elston, W. J. Blake, J. J. Collins, Nat. Rev. Genet. 6, 451 (2005).
- 23. M. Loreau et al., Science 294, 804 (2001).
- 24. D. F. Flynn, N. Mirotchnick, M. Jain, M. J. Palmer, S. Naeem, Ecology 92, 1573 (2011).
- 25. H. B. Fraser, A. E. Hirsh, G. Giaever, J. Kumm, M. B. Eisen, PLoS Biol. 2, e137 (2004).
- 26. H. L. True, S. L. Lindquist, Nature 407, 477 (2000).
- 27. J. M. Raser, E. K. O'Shea, Science 304, 1811 (2004).
- 28. K. Lewis, Nat. Rev. Microbiol. 5, 48 (2007).
- 29. A. M. Abulafi, N. S. Williams, Br. J. Surg. 81, 7 (1994).
- 30. J. M. Raser, E. K. O'Shea, Science 309, 2010 (2005).

Acknowledgments: We thank L. Gibson, A. Khandani, and P. Penttila for experimental support and members of the Dick lab, especially M. Doedens, J. Wang, M. Milyavsky, and E. Laurenti for technical support and critical assessment of this work, as well as UHN biobank for specimens, the Clinical Applications of Core Technology (Affymetrix) Laboratory of the Hartwell Center for Bioinformatics and Biotechnology of St. lude Children's Research Hospital, and the American Lebanese Syrian Associated Charities of St. Jude Children's Research Hospital, Supported by Genome Canada through the Ontario Genomics Institute, Ontario Institute for Cancer Research and a Summit Award with funds from the province of Ontario, the Canadian Institutes for Health Research, the Netherlands Organisation for Scientific Research, NIH grant R21 CA149990-01, a Canada Research Chair, the Princess Margaret Hospital Foundation, and the Ontario Ministry of Health and Long Term Care (OMOHLTC). The views expressed do not necessarily reflect those of the OMOHLTC.

Supplementary Materials

www.sciencemag.org/cgi/content/full/science.1227670/DC1 Materials and Methods Supplementary Text Figs S1 to S17

Tables S1 to S13 References (31-56)

19 July 2012; accepted 26 November 2012 Published online 13 December 2012: 10.1126/science.1227670

Gut Microbiomes of Malawian Twin Pairs Discordant for Kwashiorkor

Michelle I. Smith, 1* Tanya Yatsunenko, 1* Mark J. Manary, 2,3,4 Indi Trehan, 2,3 Rajhab Mkakosya, 5 Jiye Cheng,¹ Andrew L. Kau,¹ Stephen S. Rich,⁶ Patrick Concannon,⁶ Josyf C. Mychaleckyj,⁶ Jie Liu,⁷ Eric Houpt,⁷ Jia V. Li,⁸ Elaine Holmes,⁸ Jeremy Nicholson,⁸ Dan Knights,^{9,10}† Luke K. Ursell,¹¹ Rob Knight,^{9,10,11,12} Jeffrey I. Gordon¹‡

Kwashiorkor, an enigmatic form of severe acute malnutrition, is the consequence of inadequate nutrient intake plus additional environmental insults. To investigate the role of the gut microbiome, we studied 317 Malawian twin pairs during the first 3 years of life. During this time, half of the twin pairs remained well nourished, whereas 43% became discordant, and 7% manifested concordance for acute malnutrition. Both children in twin pairs discordant for kwashiorkor were treated with a peanut-based, ready-to-use therapeutic food (RUTF). Time-series metagenomic studies revealed that RUTF produced a transient maturation of metabolic functions in kwashiorkor gut microbiomes that regressed when administration of RUTF was stopped. Previously frozen fecal communities from several discordant pairs were each transplanted into gnotobiotic mice. The combination of Malawian diet and kwashiorkor microbiome produced marked weight loss in recipient mice, accompanied by perturbations in amino acid, carbohydrate, and intermediary metabolism that were only transiently ameliorated with RUTF. These findings implicate the gut microbiome as a causal factor in kwashiorkor.

alnutrition is the leading cause of child mortality worldwide (1). Moderate acute malnutrition (MAM) refers to simple wasting with a weight-for-height z (WHZ) score between two and three standard deviations below the median defined by World Health Organization (WHO) Child Growth Standards (2, 3). Severe acute malnutrition (SAM) refers to either marasmus, which is extreme wasting with WHZ scores less than -3, or kwashiorkor, a virulent form of SAM characterized by generalized edema, hepatic steatosis, skin rashes and ulcerations, and anorexia (4, 5). The cause of kwashiorkor remains obscure. Speculation regarding its pathogenesis has focused on inadequate protein intake and/or excessive oxidative stress, but substantial evidence to refute these hypotheses has come from epidemiologic surveys and clinical trials (6–9). Our comparative metagenomic study of the gut microbiomes of 531 healthy infants, children, and adults living in the United States, Venezuela, and Malawi revealed a maturational program in which the proportional representation of genes encoding functions related to micro- and macronutrient biosynthesis and metabolism changes during postnatal development (10). Together, these observations give rise to the following testable hypotheses: (i) The gut microbiome provides essential functions needed for healthy postnatal growth and development; (ii) disturbances in microbiome assembly and function (for instance, those prompted by